

1 Regioselective S_N2 -Type Reaction for the Oriented and Irreversible 2 Immobilization of Antibodies to a Glass Surface Assisted by 3 Boronate Formation

4 Avijit K. Adak,* Kuan-Ting Huang, Pei-Jhen Li, Chen-Yo Fan, Po-Chiao Lin, Kuo-Chu Hwang,
5 and Chun-Cheng Lin*



Cite This: <https://dx.doi.org/10.1021/acsabm.0c00700>



Read Online

ACCESS |



Metrics & More

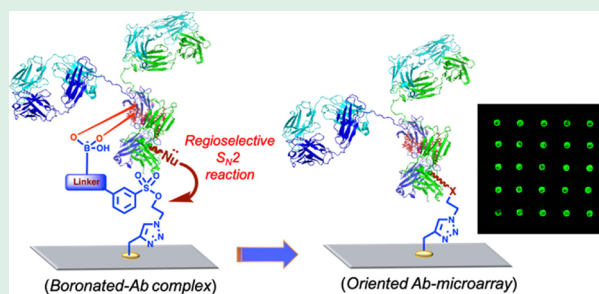


Article Recommendations



Supporting Information

6 **ABSTRACT:** Antibodies have exquisite specificities for molecular
7 recognition, which have led to their incorporation into array sensors
8 that are crucial for research, diagnostic, and therapeutic applications.
9 Many of these platforms rely heavily on surface-bound reactive groups
10 to covalently tether antibodies to solid substrates; however, this
11 strategy is hindered by a lack of orientation control over antibody
12 immobilization. Here, we report a mild electrophilic phenylsulfonate
13 (tosylate) ester-containing boronic acid affinity ligand for attaching
14 antibodies to glass slides. A high level of antibody coupling located
15 near the Fc region of the boronated antibody complex could be
16 achieved by the proximal nucleophilic amino acid driven substitution
17 reaction at the phenylsulfonate center. This enabled the full-length antibodies to be permanently tethered onto surfaces in an
18 oriented manner. The advantages of this strategy were demonstrated through the individual and multiplex detection of protein and
19 serum biomarkers. This strategy not only confers stability to the immobilized antibodies but also presents a different direction for the
20 irreversible attachment of antibodies to solid supports in an orientation-controlled way.



21 **KEYWORDS:** boronic acid, oriented immobilization, biomarker detection, antibody microarray, boronate formation

22 ■ INTRODUCTION

23 Antibodies (Abs), most commonly immunoglobulin G (IgG)
24 isotypes, are a special class of macromolecular glycoprotein
25 with unmatched versatility for molecular recognition due to
26 their unique selectivity for both synthetic and natural epitopes,
27 which is often with high affinity.¹ Besides their traditional use
28 as therapeutic drugs and labeled detection probes in assays
29 such as western blot, flow cytometry, and immunohistochem-
30 istry, Abs are also the primary components of many
31 immunosensor-based applications including screening of
32 microbial pathogens, disease identification, point-of-care
33 clinical analyses, and various biomarker detection.² The
34 majority of these applications require Abs to be essentially
35 conjugated onto solid supports (e.g., microtiter plates,
36 nanoparticles, and glass slides) while preserving analyte-
37 binding activity.³ The immobilization of Abs is complicated
38 by their chemical complexity as the reactivity of amino acid
39 residues varies greatly according to their position in the three-
40 dimensional structure. One of the main challenges for Ab
41 immobilization methods is finding chemical strategies that
42 allow for controlled immobilization of Abs while ensuring
43 retention of their functionality.⁴

44 Traditionally, Abs have been immobilized on detection
45 surfaces, both non-covalently by means of physical adsorption

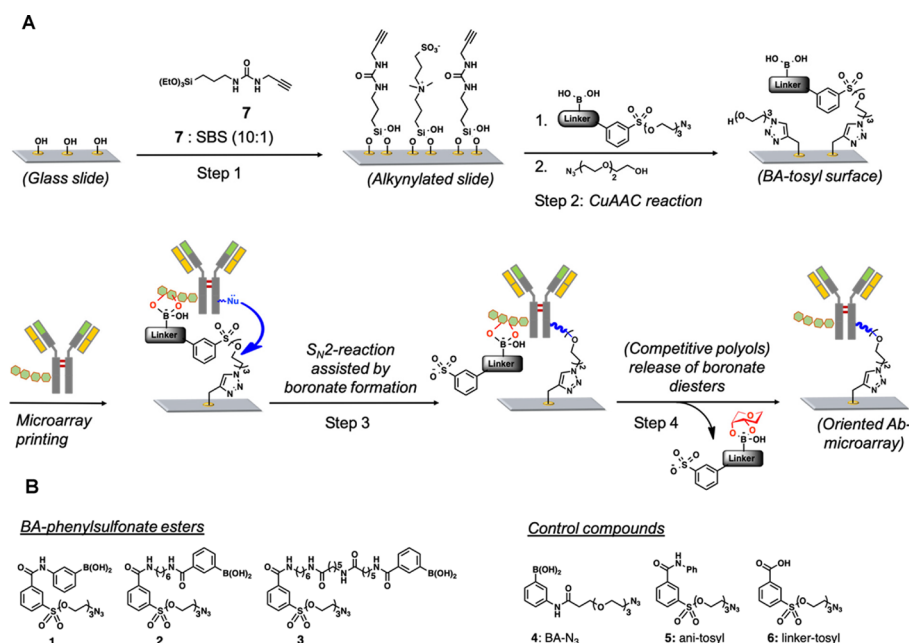
and covalently by random amine-coupling methods.⁵ Although 46
these straightforward strategies do not require extensive Ab 47
modification, multiple sites for attachment of the Ab to the 48
surface leads to an array in which Abs have a random 49
orientation, causing inaccessibility of antigen-binding sites.⁶ In 50
addition, IgGs are often produced either in complex biological 51
media such as ascites or fluids or supplied in amine-containing 52
buffers (e.g., Tris-based), supplement proteins, or stabilizers 53
such as bovine serum albumin (BSA). Such formulations could 54
limit the application of carbodiimide (e.g., EDC)/N-hydrox- 55
ysuccinimide (NHS)-based coupling strategy. Alternatively, 56
site-specific covalent immobilization on solid substrates 57
displays both a markedly higher capacity to bind antigens 58
and more reproducible Ab activity.⁷ 59

A popular site-specific conjugation method commonly 60
utilizes thiol groups generated by the reduction of native 61
disulfide bonds of IgG heavy chains.⁷ Notably, although the 62

Received: June 8, 2020

Accepted: August 31, 2020

Published: August 31, 2020

Scheme 1. Oriented and Irreversible Ab Immobilization on a BA–Phenylsulfonate-Coated Glass Slide through Boronate Diester Formation^a

^a(A) Schematic representation of the surface functionalization by CuAAC reaction using BA–phenylsulfonate on an alkyne-terminated glass surface followed by regioselective S_N2-type reaction between nucleophile amino acid side chains from the Fc region of the boronated IgG complex and surface-bound phenylsulfonate ester groups resulting in irreversible attachment of a full-length Ab upon boronate formation. (B) Structures of BA-containing phenylsulfonate ester probes (1–3) and control compounds (4–6) used in this study.

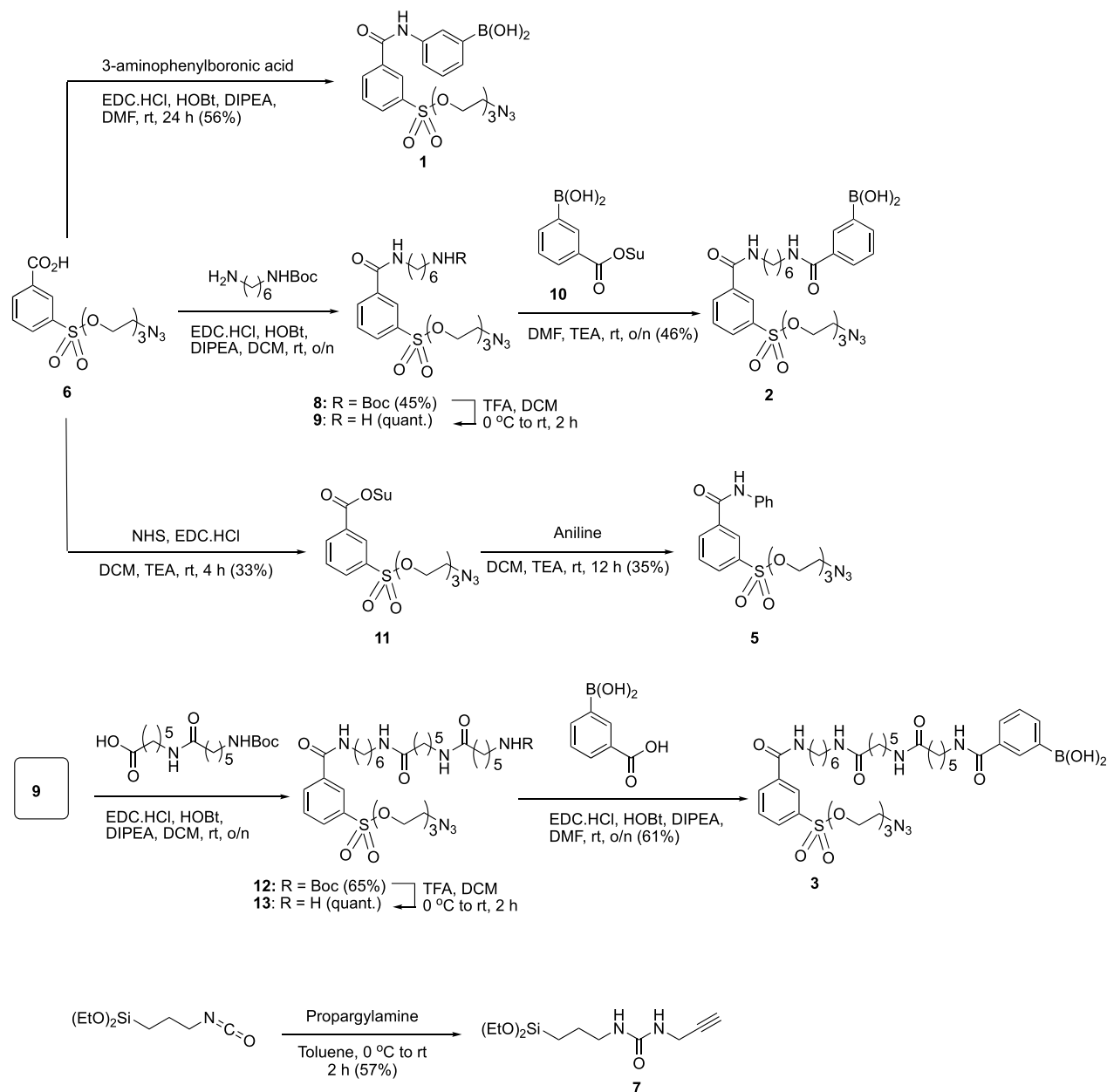
63 cysteine residue provides sites for uniform orientation, the
64 requirements of harsh reaction conditions, which impact Ab
65 tertiary structure and function, are inevitable.⁸ Furthermore,
66 thiolated Abs have the additional shortcoming of being prone
67 to undesired disulfide bond formation.⁹ To alleviate these
68 problems, natural IgG-binding proteins, such as Protein A,
69 Protein G, or Protein L, which only bind to the fragment
70 crystallizable (Fc) region of IgG have been exploited for site-
71 specific and non-covalent immobilization.¹⁰ However, the non-
72 covalent interaction between IgG and Fc protein receptors
73 renders these complexes bio-unstable. In addition, orientation
74 control of Protein A or G during immobilization is an initially
75 critical event for obtaining an ideally oriented IgG anchor.
76 Incorporating photoactivatable groups into Protein G binding
77 domain¹¹ or mutated Protein Z,¹² derived from the B domain
78 of Protein A, results in a covalent and site-specific crosslink
79 onto the Fc region of IgG upon UV light activation.¹³ The
80 major downside of this technique is the difficulty in
81 incorporating the photophores into IgG-binding proteins,
82 which requires either synthesis of peptides or post-translational
83 modification, both of which are not always straightforward
84 since sophisticated chemical and genetic modifications are still
85 involved. Despite their aforementioned shortcomings, these
86 immobilization techniques have been illustrative in showcasing
87 that controlled orientation holds higher Ab functional
88 activities.

89 The vicinal diols of Ab oligosaccharides can be oxidatively
90 cleaved with NaIO₄ to generate reactive aldehydes that can
91 react with amines or hydrazides for site-specific and covalent
92 conjugation.¹⁴ However, the requisite chemical treatments on
93 IgG are likely to trigger the possibility of significant oxidative
94 side reactions including Ab cross-linking and protein
95 denaturation. Chemical strategies that do not require prior

Ab modification capable of directing antigen capture sites away
96 from the immunosensor surface in a controlled manner are
97 highly challenging. Boronic acids (BAs) provide a simple
98 solution to this problem by targeting the Fc N-glycans of IgG
99 essentially in an oriented manner.¹⁵ 100

The C_H2 domains of all IgG heavy chains have conserved
101 glycosylation with a complex biantennary glycan at each
102 Asn297 residue.¹⁶ The intrinsic chemoselective interactions
103 between BAs and 1,2- or 1,3-diol-containing compounds are
104 sufficiently strong, enabling binding of saccharides,¹⁷ including
105 those in the glycocalyx¹⁸ in millimolar to submillimolar levels
106 but resulting in reversible single-pair interactions in aqueous
107 environments. Despite their long-standing applications in
108 carbohydrate sensing,¹⁷ pendant BAs were recently used as
109 carriers for proteins,¹⁹ capture and release of cancer cells,²⁰
110 protein modification,²¹ and determination of intracellular
111 sialyltransferase activity.²² Furthermore, the boronate-affinity-
112 based molecular imprinting approach has recently attracted
113 tremendous attention for imprinting and assaying glycopro-
114 teins.²³ The controllable and homogeneous orientation of the
115 surface-immobilized Abs is beneficial for applications in which
116 array detection sensitivity and reproducibility are an important
117 issue.^{24–26} However, reversible binding of boronate groups
118 suffers from the risk of potential protein release from
119 glycoprotein-bound complexes, which may impact protein
120 function of the array sensor.²⁷ In this regard, we incorporated a
121 photoaffinity group into the BA-based capturing ligand for
122 attaching Abs irreversibly to glass slides²⁸ and to magnetic
123 nanoparticles,²⁹ which yields higher levels of Ab immobiliza-
124 tion and antigen detection sensitivity.²⁸ Consequently,
125 generating new strategies for oriented and covalent Ab
126 microarrays without prior Ab modification and without
127 compromising assay detection capabilities are highly desirable. 128

Scheme 2. Synthesis of 1–3, 5, and 7



129 In this paper, we report a proximity-driven nucleophilic
 130 substitution ($\text{S}_{\text{N}}2$) reaction for the direct and oriented
 131 immobilization of Abs to glass slides by using BA ligands
 132 comprising a mild electrophile, phenylsulfonate (tosylate) ester
 133 group (Scheme 1A). The Ab conjugation proceeds without the
 134 use of additional reagents and, importantly, enables irreversible
 135 attachment to the BA-presenting surfaces. The advantage of
 136 this strategy for fabricating an Ab microarray is highlighted
 137 through the detection of biomarkers, serum amyloid P
 138 component (SAP), and C-reactive protein (C-RP). In addition
 139 to improving stability and Ab orientation to the solid supports,
 140 this new immobilization strategy represents a promising
 141 platform for multiplex detection of protein biomarkers in
 142 serum.

RESULTS AND DISCUSSION

Selection of BA–Phenylsulfonate Ester Probes.

Previous investigations in our laboratory have demonstrated
 the importance of oriented immobilization of Abs including
 Fc-fused protein on BA-presenting planar and metal nano-
 particle surfaces, the binding sites of which should be kept
 available for the incoming analyte.^{30–32} The formation of
 boronate diester has many attributes, including simplicity of
 the reaction, i.e., no catalyst required and biorthogonality. BAs
 complex biological diols with apparent low affinity and
 reversibility as well as functional groups such as α -amino
 acids and ϵ -amino acids; other isolated thiol groups present
 within the (bio)molecules are not involved in the inter-
 actions.³³ It has been assumed that the complementary affinity
 interactions for the purpose of oriented and irreversible
 immobilization can be extended to BA-based probes

159 containing nucleophilic side-chain-residue-specific electrophilic
160 phenylsulfonate ester group.

161 The S_N2 -type coupling reaction of the reactive tosylate
162 groups themselves offers proven compatibility with labeling of
163 numerous biomolecules, including endogenous proteins,
164 lectins, and glycoproteins on cells.³⁴ This generality in other
165 contexts suggests the intriguing possibility that a direct
166 coupling of a full-length antibody could be expanded to the
167 production of functional antibody microarrays. The suitability
168 of BA–tosylate-functionalized surfaces has been demonstrated
169 before for protein immobilization, but Ab microarray
170 fabrication has not been explored.^{35,36} Many side-chain
171 nucleophiles including Tyr, His, Glu, Asp, and Cys are reactive
172 toward the tosylate group.³⁴ We anticipated that the proper
173 oriented immobilization of an intact IgG could be possible by
174 S_N2 substitution utilizing Fc oligosaccharide of IgG as a
175 temporary scaffold and nucleophiles specifically at the non-
176 antigenic Fc region of the boronated Ab complex located far
177 away from the antigen-binding fragment (Fab), which then
178 reacts with phenylsulfonate and forms a covalent bond. To test
179 this hypothesis, BA-containing phenylsulfonate ester probes
180 1–3 were synthesized (Scheme 1B).

181 Scheme 2 describes the synthesis for the preparation of BA-
182 containing phenylsulfonate ester probes (1–3), tosylate 5, and
183 alkyne triethoxysilane 7. We used acid 6, a common building
184 block for the synthesis of tosylates 1–3, and 5. Briefly, EDC/
185 HOBt-mediated amide coupling reaction between 6 (see the
186 Supporting Information for its synthesis) and a commercially
187 available 3-aminophenylboronic acid gave BA–phenylsulfonate
188 ester 1 in 56% yield. For the synthesis of 2, a six-carbon spacer
189 *N*-Boc-1,6-hexanediamine was installed first to produce 8
190 (45%). Removal of Boc-protecting group (TFA, DCM, 0 °C, 2
191 h) in 8 generated an amine (9), which was, without
192 purification, coupled with *N*-hydroxysuccinimidyl (OSu)-
193 activated ester 10 (see the Supporting Information for its
194 synthesis) to yield 2 (46%). The amine 9 was converted with a
195 relatively longer linker 6-[(6-[[*tert*-butoxycarbonyl]amino]-
196 hexanoyl)amine]hexanoic acid²⁸ using EDC and HOBt as
197 the coupling reagents to yield 12 (65%). The latter was
198 submitted to Boc deprotection (TFA, DCM, 0 °C, 2 h), and
199 the resulting amine reacted with 3-aminophenylboronic acid
200 using EDC and HOBt as the coupling reagents, affording 3 in
201 61% yield. For the synthesis of 5, acid 6 was converted to an
202 activated ester 11 followed by coupling with aniline. The
203 alkyne triethoxysilane 7 was obtained by the formation of a
204 urea-linkage using (triethoxysilyl)propyl isocyanate and
205 propargylamine in toluene in 57% yield. Compound 4 was
206 prepared as reported previously.³²

207 **Preparation of BA–Phenylsulfonate Ester Function-
208 alized Glass Slides.** For the preparation of BA–phenyl-
209 sulfonate ester modified surfaces for Ab immobilization, mixed
210 monolayer-protected glass slides were prepared first using an
211 alkyne triethoxysilane (7; Scheme 1, step 1). We introduced a
212 freshly prepared 10 mol % aqueous solution of sulfobetaine
213 siloxane (SBS),³⁷ a zwitterion used as an additive to effect
214 homogeneous and monolayer-type surface coverage with 7 (10
215 mM in DMSO) during glass slide functionalization (see Figure
216 S1 for details). The sulfobetaine, an antifouling zwitterion, was
217 introduced as a matrix to suppress non-specific absorption of
218 protein.³⁷ A mixture of 7/SBS (10/1 mole ratio) was used to
219 functionalize the glass surface by silanization. The Cu(I)-
220 catalyzed azide–alkyne cycloaddition (CuAAC) for the
221 functionalization of solid supports including nanoparticles

with BAs was reported.^{38,39} The CuAAC reaction was then
performed (Scheme 1A, step 2) to conjugate azido-modified
BA–phenylsulfonate esters by using a solution of $CuSO_4$,
sodium ascorbate, and tris(3-hydroxypropyltriazolylmethyl)
amine (THPTA).⁴⁰ The slides were further exposed to an
azido-linked tri(ethylene glycol) (10 mM) under similar click
reaction conditions to consume the remaining alkyne groups
and to further improve the hydrophilicity of the surface.
Subsequently, the covalent immobilization of native Ab was
performed on this BA–phenylsulfonate-presenting platform.

Characterization of Surface-Bound Abs. X-ray photo-
electron spectroscopy (XPS), atomic force microscopy (AFM),
and time-of-flight secondary-ion mass spectrometry (TOF-
SIMS) were applied to characterize the presence of IgG on the
BA-phenylsulfonate ester (2)-coated surface. As shown in
Figure 1, the curve fitted high-resolution C 1s spectrum

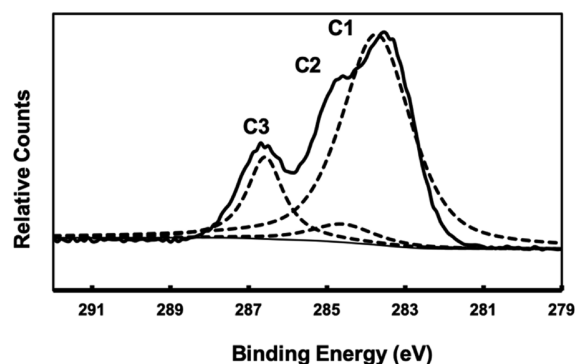


Figure 1. Curve-fitted high-resolution XPS C 1s spectrum of the BA-phenylsulfonate ester (2)-coated surface after Ab immobilization.

showed three major peaks: 283.5 eV for the aliphatic
hydrocarbons C–C/C–H, 284.7 eV for carbon bound to N
or O, and a peak at 286.6 eV corresponding to the amide
carbon of the protein.⁴¹ In addition, an appreciable enhance-
ment of N peak from 2.5% to 12.5% located at the binding
energy of ~ 398.8 eV was observed (Table 1 and Figure S2),

Table 1. XPS Atomic Concentrations of the Samples before and after IgG Immobilization

	XPS atomic concentration (at %)			
	[C]	[O]	[N]	[N]/[C]
2-coated surface	26.79	70.88	2.53	9.4
2-coated surface + IgG	53.3	34.14	12.56	23.5

indicating the presence of N (from IgG) on the 2-coated
surface, consistent with a previous report.⁴² In addition, the
ratio of N/C was increased from 9.4 to 23.5, further supporting
the presence of protein on the surface after Ab immobilization.
The XPS survey spectra of 2-coated surface before and after
IgG immobilization are shown in Figure S2. The quantitative
XPS surface analysis (sampling depth of approximately 10 nm)
also suggested that the IgG molecule was successfully
immobilized onto the 2-coated surface.

The surface morphologies of the BA–phenylsulfonate ester
(2)-coated slide and followed by Ab immobilized slide were
determined by AFM. As shown in Figure 2A, a typical RMS
roughness of 3.69 nm was observed for the BA-coated surface,
suggesting the formation of aggregates after chemical
derivatization of alkyne glass slides with BA–phenyl-

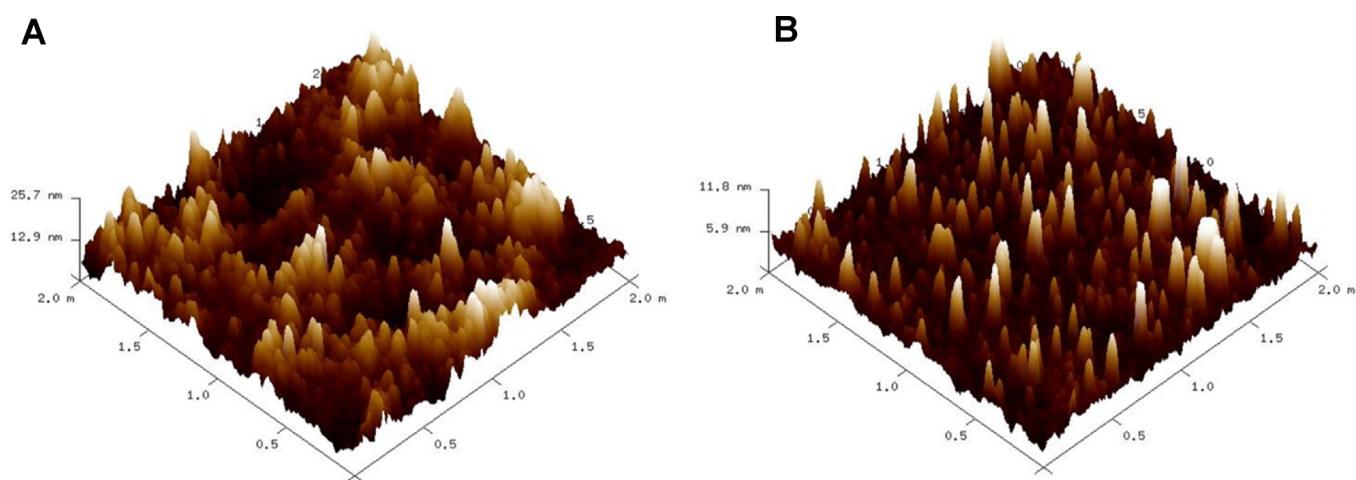


Figure 2. AFM three-dimensional tapping mode topographic image of the BA-phenylsulfonate ester (2)-coated surface (A) before and (B) after Ab immobilization. Scanning area = $2 \times 2 \mu\text{m}^2$.

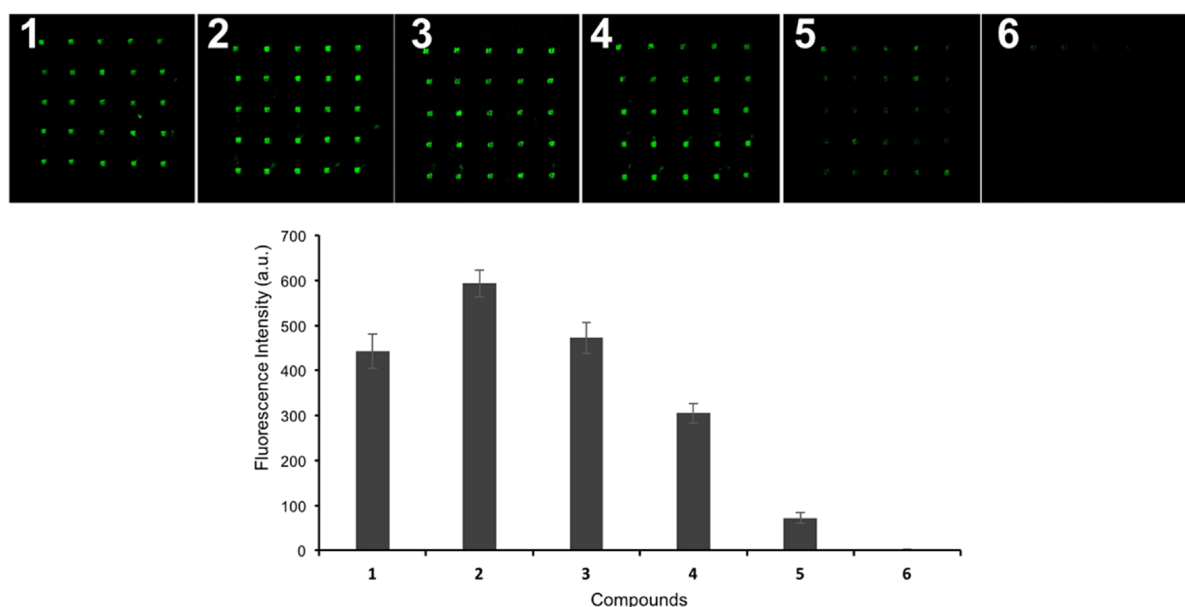


Figure 3. Oriented and irreversible Ab immobilization on BA-phenylsulfonate ester-coated surfaces. The h-IgG ($1.6 \mu\text{M}$) was immobilized on BA-phenylsulfonate esters (1–3) and control-compound (4–6)-functionalized surfaces (see the [Experimental Section](#)). The fluorescence signals were visualized with anti-h IgG (Fc-specific)-Cy3 Ab. Corresponding fluorescence images at each indicated substrates are shown on top. Mean signals and error bars representing standard deviations (SD) from a 5×5 element array for each substrate are shown.

259 sulfonate ester (2) by the CuAAC reaction. The observed
 260 roughness can also be rationalized by the multilayer deposition
 261 of alkoxy silane used for silanization process, which is known to
 262 produce larger aggregates during surface functionalization.⁴³
 263 However, Ab microarray fabrication on BA-phenylsulfonate
 264 ester-modified surfaces produced with much low roughness
 265 (Figure 2B). Because of the more compact IgG layer, a
 266 decreased RMS value, 1.57, was observed, which is comparable
 267 to that of a BA-containing zwitterionic polymer-modified
 268 silicon wafer.²⁵ The observed height of approximately 10 nm in
 269 the AFM image corresponds well with the end-on oriented
 270 IgG.⁴⁴ These data indicate that Ab molecules could be oriented
 271 onto the surface by BA affinity ligand and is expected to
 272 perform an enhanced Ab-antigen binding event.

273 We also used ToF-SIMS for characterizing protein
 274 orientation on the surface. It was reported that the ToF-
 275 SIMS technique is capable of discerning amino acid peaks

specific to either the Ab Fab or Fc domains.^{43,45,46} In one
 276 study, this was achieved by the ratios of certain ion fragments
 277 that are characteristics of the IgG.⁴⁵ The Fab prevalent amino
 278 acid ion fragments, $\text{C}_2\text{H}_6\text{NO}^+$ (m/z 60.04 for Ser) and
 279 $\text{C}_3\text{H}_6\text{N}^+$ (m/z 56.04 for Lys), and Fc prevalent amino acid ion
 280 fragments, $\text{C}_8\text{H}_{10}\text{N}^+$ (m/z 120.08 for Phe) and $\text{C}_7\text{H}_7\text{O}^+$ (m/z
 281 107.05 for Tyr), were used for tracking IgG orientation on the
 282 BA-phenylsulfonate ester (2)-coated surface. The Ab micro-
 283 array produced by random Schiff's base formation was used as
 284 a reference. As shown in Figure S3, the ToF-SIMS peak
 285 intensity ratio of the Lys/Ser peak decreased as expected and
 286 also a reduction of the peak intensity ratio of the Tyr/Phe peak
 287 was observed. These results indicate greater exposure of Fab
 288 domain outwardly to the surface when bound to BA compared
 289 with the random immobilization method. Although relative
 290 changes in peak intensity ratios are useful in distinguishing
 291 protein domains, a combination of ToF-SIMS and principal
 292

293 component analysis method could provide comprehensive
294 overview of BA surface-immobilized Ab orientation to validate
295 these data.⁴⁷

296 Oriented and Irreversible Immobilization of Ab on 297 BA–Phenylsulfonate Ester Functionalized Glass Slides.

298 We selected h-IgG as a model Ab to establish the proximity-
299 driven S_N2 reaction for covalent and irreversible immobiliza-
300 tion. The h-IgG (1.6 μM in 20 mM HEPES buffer containing
301 150 mM NaCl and 0.05% Tween20, pH 8.5) was printed on
302 BA–phenylsulfonate ester-coated surfaces. The printed slides
303 were incubated in a humidified chamber for 12 h to allow
304 boronate formation and to effect a regioselective substitution
305 reaction with the nucleophiles in close proximity to the
306 boronated IgG complex (Scheme 1A, step 3). After washing of
307 the slides to remove unbound Abs followed by blocking with
308 dextran (100 μM containing 1% BSA), a fluorescent signal was
309 generated by exposure to a solution containing anti-h IgG (Fc-
310 specific)-Cy3 Ab (1 μg/mL).

311 As shown in Figure 3, BA–phenylsulfonate ester 2 showed a
312 better level of Ab immobilization compared with the other two
313 phenylsulfonate esters 1 and 3. BA ligand separated by a short
314 spacer allows it to be positioned appropriately relative to the
315 Ab surface, enabling key S_N2 substitution by the nucleophilic
316 amino acid residue nearby. However, BA derivative 4, which
317 lacks the reactive phenylsulfonate ester group, produced an
318 approximately 1.94-fold lower signal corresponding to that of
319 2, highlighting the importance of irreversible Ab conjugation in
320 the BA–phenylsulfonate ester-based immobilization strategy
321 through a regioselective S_N2-type reaction. The control slide
322 coated with a phenyl-substituted tosylate 5, which lacks the
323 affinity head group, generated a significantly lower (approx-
324 imately 8.3-fold) Ab signal compared to BA–phenylsulfonate
325 ester 2, demonstrating the necessity of BA affinity ligand. An
326 additional control slide using an unsubstituted tosylate linker 6
327 produced no apparent detectable signal, thereby hindering the
328 essential S_N2 reaction of Ab, likely because of inaccessibility to
329 the surface. These studies suggest that the simultaneous
330 presence of both the BA and phenylsulfonate ester group is
331 needed for Ab recruitment in an oriented and irreversible
332 manner. We chose BA–phenylsulfonate ester 2 for a
333 subsequent microarray fabrication study described below.

334 To find an optimal concentration for surface functionaliza-
335 tion, alkynylated glass slides were derivatized with 2 at five
336 different concentrations (1, 10, 25, 50, and 100 mM), but the
337 assay was otherwise run in a similar manner. As shown in
338 Figure S4, a maximum fluorescence signal was produced at
339 probe concentrations of 10–25 mM, above which the signal
340 intensity tended to decrease because of boroxine formation, as
341 suggested previously.²⁹ Additionally, effects of Ab concen-
342 tration (0.2–6.6 μM) and time of boronated IgG complex
343 formation (2–18 h) were evaluated by using a 2-coated surface
344 (10 mM). As shown in Figure S5, a dose-dependent response
345 in fluorescence was observed relative to the amount of treated
346 IgG, with a signal saturation between 1.6 and 3.3 μM. Notably,
347 a 12 h Ab (1.6 μM) incubation period generated a signal
348 comparable to that of a longer reaction time (18 h), indicating
349 near completion of the substitution reaction between
350 nucleophilic amino acid residues of boronated IgG complex
351 and a phenylsulfonate center (Figure S6).

352 Because of the characteristic covalent but reversible binding
353 between BAs and sugars, immobilized Abs by boronate
354 formation could compete for higher-affinity binders for
355 boron complexation and release the boronate diesters (Scheme

1A, step 4). To evaluate whether the surface Ab was 356
immobilized by a covalent bond formed by S_N2 substitution 357
or reversible boronate ester, Ab-coated slides were separately 358
incubated with D-fructose (D-Fru, 50 mM) and 5-N- 359
acetylneuraminic acid (Neu5Ac, 50 mM), which are known 360
to have a higher affinity to BAs,¹⁹ as well as a 10% solution 361
containing glycerol, a surfactant commonly used in microarray 362
applications. The binding results revealed in Figure S7 show 363
that the fluorescence intensities after 2 h exposure to sugars 364
and glycerol yielded essentially no apparent change in signals. 365
These results suggest that most, if not all, of the immobilized 366
Abs covalently attached by reaction with the electrophilic 367
phenylsulfonate center. In addition, quantitative analysis of 368
fluorescence intensities demonstrated that Ab microarrays 369
produced by oriented and irreversible immobilization on BA– 370
phenylsulfonate ester surface provides 6.7-fold higher intensity 371
compared to the microarray formed by random Schiff's base 372
formation (Figure S8), highlighting the superiority of the S_N2- 373
reaction-based oriented immobilization approach. 374

375 **Stability of Surface-Bound Abs in Serum.** To 375
determine the stability of immobilized Abs, alkynylated glass 376
slides were functionalized separately with a 10 mM solution of 377
2 and 4 by CuAAC. Figure 4 shows the fluorescence intensity 378 4

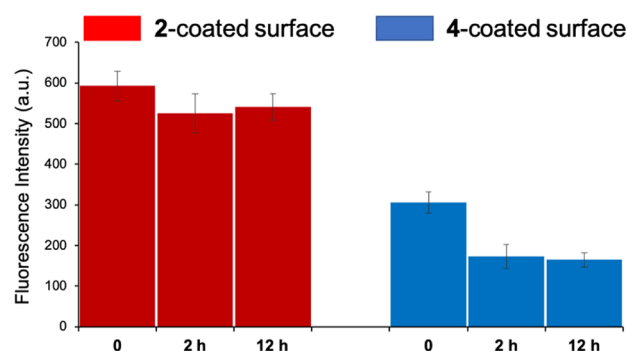


Figure 4. Stability of surface-immobilized covalent Ab microarrays from serum-induced dissociation. The h-IgG (1.6 μM) was printed on 2- and 4-coated surfaces, which was then incubated either in the absence or presence of FBS (1:1 in PBS) for 0–12 h at room temperature. The presence of the remaining surface-bound Abs was visualized by anti-h IgG (Fc-specific)-Cy3 Ab. Mean signals and the SD are shown.

379 patterns of the h-IgG (1.6 μM) immobilized onto 2- and 4- 379
coated surfaces depending on the treatment of fetal bovine 380
serum (FBS) for 0–12 h. The FBS induced an approximate 381
53% dissociation after 12 h of the bound Abs from the 382
microarrays produced by the 4-coated surface, indicating that 383
the reversible nature of the boronate diesters is more 384
susceptible to serum-mediated dissociation. Conversely, the 385
dissociation was almost completely protected from the 2- 386
coated surface, demonstrating that Ab immobilization through 387
the reactive tosylate functional group is stable in complex 388
biofluids such as serum. This provides evidence that the BA– 389
phenylsulfonate ester-mediated Ab immobilization method is 390
applicable for detecting and quantitating analytes in complex 391
biological samples (see below). 392

393 **Individual Protein and Biomarker Detection on the**
394 **BA–Phenylsulfonate Ester-Coated Surface.** Precise de- 394
tection of protein biomarkers is of considerable importance 395
because it can enable early and accurate diagnosis of diseases.⁴⁸ 396
We first illustrated the aspects of BA–phenylsulfonate ester- 397

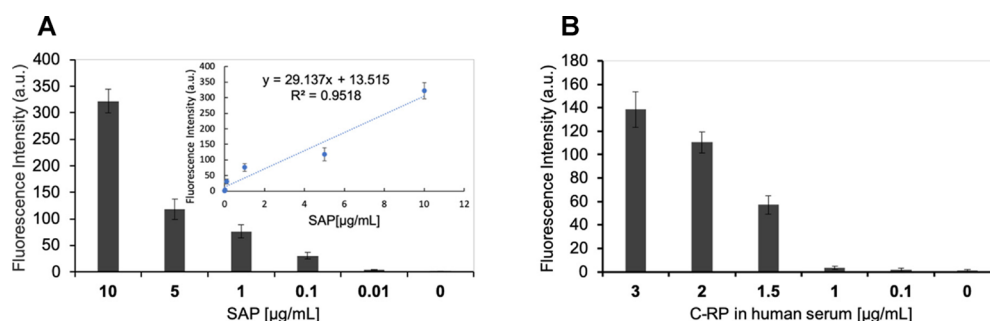


Figure 5. Functional Ab microarrays for the detection of single-protein biomarkers. Detection of (A) SAP and (B) C-RP. Anti-human C-RP and SAP capture Abs ($1.6 \mu\text{M}$), which were printed on 2-coated surfaces, incubated with various concentrations of SAP and C-RP, and visualized with corresponding biotinylated anti-CRP and SAP pAbs and streptavidin-Cy3. Inset in (A) shows the effect of SAP concentration on the fluorescence intensity. The LOD was estimated as follows: $\text{LOD} = \text{mean signal of the blank} + 3 \times \text{SD of the blank}$. Mean signals and the SD are shown.

398 coated slides by the measurement of two individual biomarker
 399 proteins, SAP and C-RP. SAP is a serum protein related to
 400 Alzheimer's disease and type 2 diabetes, and C-RP is a protein
 401 responsive to inflammation and cardiovascular disease.⁴⁹ In
 402 humans, normal plasma SAP levels are relatively stable,
 403 approximately $30\text{--}40 \mu\text{g/mL}$,⁵⁰ and remain constant during
 404 acute or chronic inflammation. However, C-RP concentrations
 405 in healthy individuals increase from less than $10 \mu\text{g/mL}$ to
 406 approximately $350\text{--}400 \mu\text{g/mL}$, depending on disease states.⁵¹
 407 For the detection of SAP, an anti-SAP Ab ($1.6 \mu\text{M}$) microarray
 408 was fabricated onto a 2-coated surface. Next, a series of SAP
 409 ($100 \mu\text{L}$) concentrations (0.01, 0.1, 1, 5, and $10 \mu\text{g/mL}$) in
 410 assay buffer (PBS buffer containing 0.005% Tween20 and 0.1%
 411 BSA, pH 7.4) were incubated with the anti-SAP Ab slide for 1
 412 h. The presence of bound protein was then evaluated by using
 413 biotinylated anti-SAP pAb (polycloned Ab) ($1 \mu\text{g/mL}$)
 414 followed by staining with Cy3-labeled streptavidin ($10 \mu\text{g}/$
 415 mL). Figure 5A shows the corresponding plot of fluorescence
 416 intensity as a function of SAP concentration from the arrayed
 417 spots. We note that the lowest analyte concentration that
 418 produces a detectable signal is $1 \mu\text{g/mL}$ (Figure 5A and Figure
 419 S9). The Ab microarray could reproducibly detect SAP
 420 concentration as low as $0.87 \mu\text{g/mL}$ ($\sim 34 \text{ nM}$); limit of
 421 detection, LOD) with coefficient of variation (%CV) ranging
 422 from 1.5% to 6.8%, well below the plasma SAP concentrations
 423 in healthy subjects. When measured in serum, a detection
 424 sensitivity of $\sim 79 \text{ nM}$ was achieved (Figure S10).

425 Following this proof of concept, we directly turned to the
 426 detection of C-RP from human serum, which was also
 427 desirable for measuring the analyst in a complex biological
 428 environment in diagnostic applications. For these studies,
 429 serum from a healthy volunteer was collected. The enzyme-
 430 linked immunosorbent assay (ELISA) estimated a total C-RP
 431 concentration of $3.0 \mu\text{g/L}$ (Figure S11), which was then
 432 diluted to produce solutions with concentrations of 0.1, 1.0,
 433 1.5, 2.0, and $3.0 \mu\text{g/mL}$ for analysis. A $100 \mu\text{L}$ portion of each
 434 solution was applied for 1 h with an anti-h C-RP Ab microarray
 435 constructed using a 2-presenting surface. Biotinylated
 436 detection of Ab for C-RP (1/100 dilution) was then applied
 437 followed by a final developing step using fluorescent Cy3-
 438 labeled streptavidin, with multiple washes in between each
 439 step. Quantifying the fluorescence intensity (Figure 5B and
 440 Figure S11) revealed a sensitivity of approximately $1.4 \mu\text{g/mL}$
 441 ($\sim 57 \text{ nM}$) (%CV ranged from 3.7% to 13.6%), which is within
 442 the critical concentration range for cardiovascular risk
 443 assessment.⁵² This detection limit was approximately seven
 444 times lower relative to that of an enzyme immunoassay.⁵³

Thus, the sensitivity achieved using a BA-phenylsulfonate
 strategy is suitable for direct detection of both biomarkers SAP
 and C-RP.

To demonstrate the generality of the developed method, the
 BA-phenylsulfonate ester-coated surface was also tested using
 a plant lectin, *Ricinus communis* Agglutinin 120 (RCA_{120}), a
 useful lectin surrogate for the biological warfare toxic agent
 ricin (Figure S12). Using an anti- RCA_{120} Ab microarray, we
 could achieve a sensitivity of $0.98 \mu\text{g/mL}$ ($\sim 8.1 \text{ nM}$), which is
 three orders of magnitude less sensitive than that of a related
 BA-photocrosslinking-based irreversible Ab immobilization
 strategy.²⁸ The lower sensitivity of the present method is
 probably due to the low reaction rate of the key $\text{S}_{\text{N}}2$ -type
 reaction during the protein immobilization step,³⁵ resulting in
 lower Ab density on the surface. Nevertheless, the current
 technique is suitable for detecting serum biomarkers in
 multiplex assay format (see below).

Detection of Multiplex Protein Biomarkers in a Spiked Serum by Using BA-Phenylsulfonate Ester Functionalized Glass Slides. Development of highly sensitive assays that can specifically target several analytes in a parallel manner by using a single sample, i.e., multiplexed, are critically important for improved disease diagnostics and discovery of biomarkers.⁵⁴ Prior to our investigation on multiplexed measurements of biomarkers in serum, we investigated the potential of Ab microarrays in mediating selective capture of three analytes. Toward this end, an Ab microarray consisting of three Abs including anti-C-RP, anti-SAP, and anti- RCA_{120} at a concentration $1.6 \mu\text{M}$ was printed on a 2-coated surface in 10 replicate spots (2×5 array format). After Ab immobilization, three different solutions of the corresponding antigens (the lowest concentration of protein that produced a detectable signal; please refer to Figures S9 and S13), each containing C-RP ($1.5 \mu\text{g/mL}$), SAP ($1 \mu\text{g/mL}$), and RCA_{120} ($1 \mu\text{g/mL}$) in diluted human serum (1:1 in PBS) in assay buffer individually or a mixture containing all these three antigens, were applied to the Ab slide for 1 h. Captured protein targets were detected by incubating respective biotinylated Abs (see the Supporting Information for details). As shown in Figure S13, each set of Ab microarrays with a particular biomarker and lectin-specific Ab responded only to the appropriate analyte solution. Figure S13 also illustrates the fluorescence intensity of all three antigens after incubation in the mixture, demonstrating that the proposed BA-phenylsulfonate-based Ab microarray can specifically capture and indicate the corresponding antigens in

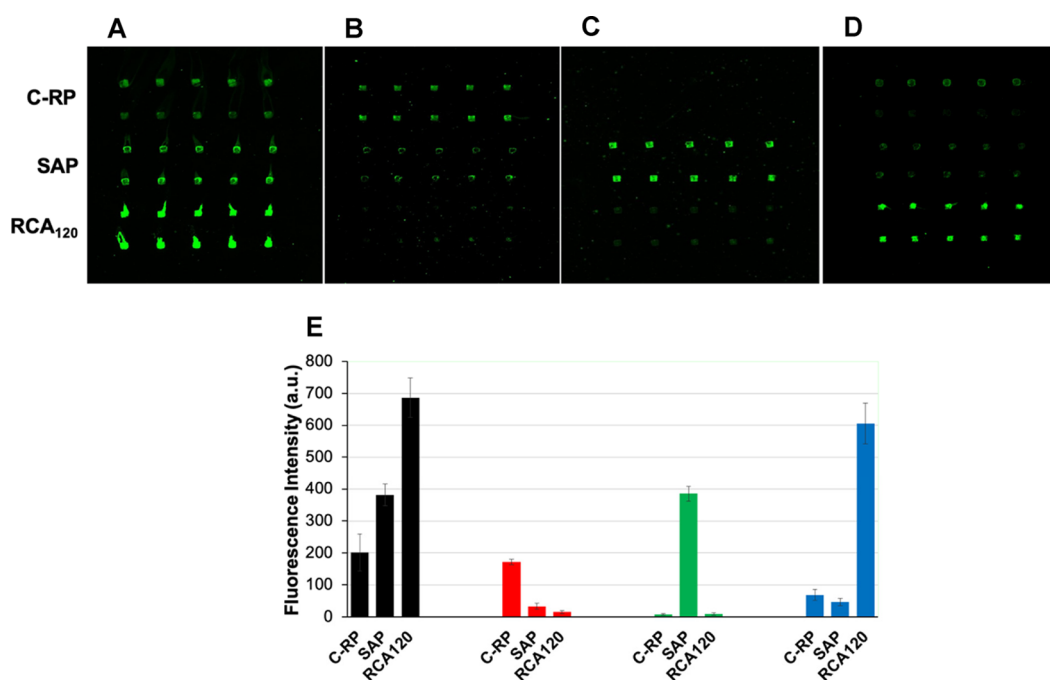


Figure 6. Multiplex detection of C-RP, SAP, and RCA₁₂₀ in serum. A microarray comprising three captured Abs targeting these analytes on a 2-coated surface was constructed: (A) One sample containing a mixture of all three analytes and three samples containing a single analyte (B) C-RP (3.0 $\mu\text{g}/\text{mL}$) in diluted serum and (C) SAP (10 $\mu\text{g}/\text{mL}$) and (D) RCA₁₂₀ (10 $\mu\text{g}/\text{mL}$) spiked in diluted FBS were applied. After analyte capture for 1 h, biotinylated reporter Abs and streptavidin-Cy3 fluorescent conjugates were used to sandwich and label the analyte in preparation for subsequent fluorescence detection. Representative fluorescence images obtained from incubation of (A) all three analytes, (B) C-RP ($p < 0.003$), (C) SAP ($p < 0.0052$), and (D) RCA₁₂₀ ($p < 0.0054$), respectively. (E) Comparison of the fluorescence signals in (A)–(D), corresponding to the multiple analyte detection (black bars) or single analyte detection (C-RP: red bars, SAP: green bars, RCA₁₂₀: blue bars). Each data point represents the mean \pm SD of the 10 captured Ab printed spots.

491 a mixture simultaneously with minimum noticeable cross-
492 interaction for these Ab-antigen combinations.

493 After establishing the feasibility of multiplexing detection in
494 buffered solution, we utilized the Ab microarray to enable the
495 simultaneous detection of three protein targets in serum. Since
496 the Ab-antigen binding affinities for all the captured Abs differ,
497 which strongly correlates with the fractional occupation sites
498 available for binding to the microarray surface, we ensured
499 equal loading of Abs (1.6 μM) onto arrayed spots with
500 incubation of a higher concentration of all three analytes in
501 serum. Diluted FBS samples (1:1 in PBS) spiked with a
502 designated concentration of SAP (10 $\mu\text{g}/\text{mL}$) and RCA₁₂₀ (10
503 $\mu\text{g}/\text{mL}$) were applied to the microarray. Because C-RP was
504 obtained from human serum, it (3.0 $\mu\text{g}/\text{mL}$) was used with no
505 added FBS in these studies. Subsequently, captured proteins
506 were simultaneously detected with respective biotin-conju-
507 gated detection Abs: C-RP pAb (1/100 dil.), SAP pAb (1 $\mu\text{g}/$
508 mL), anti-RCAI&II pAb (1 $\mu\text{g}/\text{mL}$), and streptavidin-Cy3
509 conjugates (10 $\mu\text{g}/\text{mL}$) were included in the assay buffer, as
510 described before.

511 **Figure 6B–D** represent fluorescence images, each depicting
512 three sets of captured Ab array spots, indicating successful
513 recognition of the specific protein. In addition, **Figure 6A**
514 illustrates the simultaneous capture and detection of all three
515 individual targets. We note that low cross-reactivity against
516 other proteins resulted from multiple nontargeted proteins
517 present in serum samples due to non-specific binding with anti
518 C-RP or anti-RCA₁₂₀ capture Abs arrayed spots.⁵⁵ Such a
519 nonspecific cross-reacting signal in anti-SAP Ab is insignificant.
520 However, serum-induced non-specific background signal was
521 negligible likely because of an additional protection of a

zwitterionic monolayer during glass slide functionalization. 522
With the increase in concentration, the increased levels of 523
fluorescence signal as a consequence of more analyte captured 524
on the arrayed spots resulted in higher fluorescence intensity 525
(**Figure 6E**). This demonstrates that our approach is capable of 526
simultaneously analyzing multiple targets in complex biological 527
samples. 528

529 CONCLUSIONS

In conclusion, we have established boronic acid in combination 530
with a reactive phenylsulfonate ester as a promising platform 531
for applying antibodies irreversibly to solid supports in a 532
controllable manner. The covalent attachment through 533
phenylsulfonate ester group offers a simple and robust 534
procedure for the stable immobilization of the captured 535
antibody due to its ease of preparation and use, biocompat- 536
ibility, and, most importantly, its reagentless nature, which 537
prevents the need for chemical activation of the surface. The 538
antibody microarray constructed through the BA-phenyl- 539
sulfonate ester strategy shows that both purified proteins and 540
biomarkers within the serum can be bound and are capable of 541
simultaneously capturing and detecting protein targets in 542
serum. It is likely that the developed method provides 543
opportunities for interrogating multiple protein biomarkers 544
that are amenable to diagnostic application. 545

546 EXPERIMENTAL SECTION

Materials. All starting materials and reagents were obtained from 547
commercial sources and used as received unless otherwise noted. 3- 548
(Dimethyl-(3-(trimethoxysilyl)propyl)ammonio)propane-1-sulfonate 549
(sulfobetaine siloxane, SBS) and 3-isocyanatopropyltriethoxysilane 550

551 were purchased from Gelest Inc. Bovine serum albumin (BSA), R.
552 *communis* agglutinin 120 (RCA₁₂₀), IgG from human serum, anti-
553 human IgG (Fc specific)-Cy3 Ab, monoclonal anti-C-RP Ab, dextran
554 (D-1662), and streptavidin-Cy3 conjugate were purchased from
555 Sigma-Aldrich (St. Louis, MO, USA) and used as received.
556 Unconjugated monoclonal rabbit anti-RAC (ricin alpha chain)
557 antibody was obtained from EY Laboratories. Serum Amyloid P
558 component was obtained from Calbiochem. Rabbit polyclonal Ab to
559 SAP was acquired from Thermo Scientific. Biotinylated rabbit
560 polyclonal Ab to C-RP was purchased from Abcam. Biotinylated
561 anti-human SAP polyclonal Ab was purchased from MyBiosource,
562 Inc. Biotinylated anti-RCAI & II Ab was obtained from Vector
563 Laboratories. Deionized water with a resistivity of >18 MΩ-cm was
564 obtained from an ultrafiltration system (Milli-Q, Millipore) and
565 passed through a 0.22 μm filter to remove particulate matter.

566 **Synthesis of BA-Phenylsulfonate Ester 1.** To a solution of
567 acid **6** (80 mg, 0.22 mmol, 1 equiv) and 3-aminophenylboronic acid
568 (43 mg, 0.27 mmol, 1.25 equiv) in DMF (2.0 mL) was added EDC·
569 HCl (47 mg, 0.24 mmol, 1.1 equiv), HOBt (33 mg, 0.24 mmol, 1.1
570 equiv), and DIPEA (0.092 mL, 0.51 mmol, 2.35 equiv). The reaction
571 was stirred at 25 °C for 24 h and then concentrated. The residue was
572 poured into water, and the aqueous layer was extracted twice with
573 EtOAc. The organic phase was collected and washed with saturated
574 aqueous NaCl, dried over MgSO₄, and then concentrated. The
575 residue was purified by flash silica gel column chromatography
576 (EtOAc/hexanes = 1/1) to afford **1** (60 mg, 56%). *R_f* = 0.37 (10%
577 MeOH in EtOAc/hexanes = 1/2). ¹H NMR (DMSO-*d*₆, 400 MHz):
578 δ 10.51 (br s, 1H), 8.47 (s, 1H), 8.35 (d, 1H, *J* = 8.0 Hz), 8.09 (d, 1H,
579 *J* = 7.8 Hz), 8.04 (s, 1H), 8.02 (s, 2H), 7.85 (d, 1H, *J* = 8.0 Hz), 7.83
580 (t, 1H, *J* = 8.0 Hz), 7.56 (d, 1H, *J* = 7.8 Hz), 7.33 (t, 1H, *J* = 7.8 Hz),
581 4.21 (t, 2H, *J* = 4.2 Hz), 3.60 (t, 2H, *J* = 4.2 Hz), 3.53 (t, 2H, *J* = 4.7
582 Hz), 3.48–3.41 (m, 4H), 3.37–3.27 (m, 2H). ¹³C NMR (DMSO-*d*₆,
583 100 MHz): δ 166.52, 138.77, 138.12, 137.66, 133.94 (2), 131.81,
584 131.36, 130.97 (2), 129.13, 128.17 (2), 71.58, 71.54, 71.39, 71.09,
585 69.74, 51.68. HRMS (ESI) *m/z* calcd for C₁₉H₂₂N₄O₈S⁻ [M - H]⁻
586 477.151, found 477.1249.

587 **BA-Phenylsulfonate Ester 2.** A 50 mL round bottle flask was
588 loaded with **8** (420 mg, 0.75 mmol) and placed in an ice bath. TFA
589 (20%) in CH₂Cl₂ (5 mL) was added, and the resulting solution was
590 warmed up to rt over 30 min. After being stirred for an additional 1.5
591 h, the mixture was concentrated under reduced pressure to yield an
592 oily residue. The volatiles were azeotropically removed using toluene
593 (3x10 mL). The resulting residue was dried *in vacuo* to give the amine
594 (**9**) as TFA salt (428 mg, quant.). Et₃N (0.07 mL, 0.5 mmol, 1.0
595 equiv) was added to a solution of amine (290 mg, 0.5 mmol, 1.0
596 equiv) and activated ester **10** (133 mg, 0.5 mmol, 1.0 equiv) in DMF
597 (5 mL). The resulting solution was stirred at 25 °C for overnight. The
598 reaction mixture was then concentrated, and the resulting residue was
599 redissolved in water/EtOAc. The organic layer was separated, washed
600 with saturated aqueous NaCl, dried over MgSO₄, and filtered. After
601 concentration *in vacuo*, the crude product was purified by silica gel
602 column chromatography (5–10% MeOH in CH₂Cl₂) to afford **2** (140
603 mg, 46%). *R_f* = 0.22 (10% MeOH in 1:1 EtOAc/hexanes). ¹H NMR
604 (DMSO-*d*₆, 400 MHz): δ_H = 8.79 (br s, 1H), 8.35 (br s, 1H), 8.33 (s,
605 1H), 8.21 (d, 1H, *J* = 7.6 Hz), 8.20 (s, 1H), 8.12 (s, 2H), 8.03 (d, 1H,
606 *J* = 7.8 Hz), 7.88 (d, 1H, *J* = 7.6 Hz), 7.81 (d, 1H, *J* = 7.8 Hz), 7.76 (t,
607 1H, *J* = 7.8 Hz), 7.38 (t, 1H, *J* = 7.6 Hz), 4.17 (t, 2H, *J* = 4.2 Hz),
608 3.58 (t, 2H, *J* = 4.2 Hz), 3.52 (t, 2H, *J* = 4.2 Hz), 3.45–3.43 (m, 4H),
609 3.36–3.33 (m, 2H), 3.28–3.21 (m, 4H), 1.54–1.50 (m, 4H), 1.36–
610 1.32 (m, 4H). ¹³C NMR (CD₃OD, 100 MHz): δ_C = 170.59, 167.67,
611 137.91, 137.10, 135.00, 134.96, 133.54 (2), 131.51, 130.89, 129.88,
612 128.68, 127.75 (2), 71.49, 71.44, 71.31, 71.02, 69.64, 51.62, 41.06,
613 40.81, 30.38, 30.22, 27.63, 27.60. HRMS (ESI) *m/z* calcd for
614 C₂₆H₃₆BN₅O₉SNa [M + Na]⁺ 628.2225, found 628.2224.

615 **BA-Phenylsulfonate Ester 3.** A 25 mL round bottle flask was
616 loaded with **12** (60 mg, 0.076 mmol) and placed in an ice bath. TFA
617 (20%) in CH₂Cl₂ (2 mL) was added, and the resulting solution was
618 warmed up to 25 °C over 30 min. After being stirred for an additional
619 1.5 h, the mixture was concentrated under reduced pressure to yield
620 an oily residue. The volatiles were azeotropically removed using

toluene (3x5 mL). The resulting residue was dried *in vacuo* to give the
621 amine (**13**) as TFA salt (61 mg, quant.). DIPEA (0.04 mL, 0.21
622 mmol, 3.0 equiv) was added to a solution of above amine **13** (61 mg,
623 0.076 mmol, 1.0 equiv), 3-carboxyphenylboronic acid (12 mg, 0.076
624 mmol, 1.0 equiv), EDC·HCl (16 mg, 0.084 mmol, 1.1 equiv), and
625 HOBt (12 mg, 0.084 mmol, 1.1 equiv) in DMF (2 mL). The reaction
626 mixture was allowed to stir at ambient temperature for 12 h. The
627 reaction mixture was then concentrated *in vacuo*, and the resulting
628 residue was redissolved in water/EtOAc. The organic layer was
629 separated, washed with saturated aqueous NaCl, dried over MgSO₄,
630 and filtered. After concentration *in vacuo*, the crude product was
631 purified by flash column chromatography (20% MeOH in CH₂Cl₂) to
632 yield **3** (15 mg, 61%). *R_f* = 0.25 (20% MeOH in CH₂Cl₂). ¹H NMR
633 (CD₃OD, 400 MHz): δ_H = 8.36 (s, 1H), 8.16 (d, 1H, *J* = 7.8 Hz),
634 8.07 (d, 1H, *J* = 7.8 Hz), 7.96–7.92 (m, 1H), 7.82–7.79 (m, 2H),
635 7.73 (t, 1H, *J* = 7.8 Hz), 7.41 (t, 1H, *J* = 7.8 Hz), 4.85 (br s, 1H), 4.22
636 (t, 2H, *J* = 4.4 Hz), 3.67 (t, 2H, *J* = 4.4 Hz), 3.60 (t, 2H, *J* = 4.4 Hz),
637 3.55–3.52 (m, 4H), 3.41–3.37 (m, 4H), 3.36–3.32 (m, 2H), 3.17–
638 3.12 (m, 4H), 2.21–2.14 (m, 4H), 1.65–1.62 (m, 6H), 1.53–1.47 (m,
639 4H), 1.41–1.37 (m, 10H). ¹³C NMR (CD₃OD, 100 MHz): δ_C = 640
176.04, 176.02, 170.74, 167.81, 138.11, 137.71, 137.21, 133.56 (2),
641 131.60, 130.94 (2), 129.57, 128.65, 127.85 (2), 71.61, 71.52, 71.43,
642 71.14, 69.75, 51.73, 41.10, 40.78, 40.21, 40.17, 37.01, 39.99, 30.32,
643 30.31, 30.19, 30.08, 27.67, 27.60, 27.56, 27.51, 26.74, 26.70. HRMS
644 (ESI) *m/z* calcd for C₃₈H₅₈BN₅O₁₀SNa [M - N₂ + Na]⁺ 826.3844,
645 found 826.3835. 646

647 **Aniline-Sulfonate Ester 5.** To a solution of ester **11** (100 mg,
648 0.22 mmol, 1 equiv) and freshly distilled aniline (40 mg, 0.44 mmol,
649 2.0 equiv) in CH₂Cl₂ (5 mL) was added Et₃N (0.064 mL, 0.44 mmol,
650 2.0 equiv). The reaction mixture was allowed to stir at ambient
651 temperature for 12 h. The reaction mixture was then concentrated *in*
652 *vacuo*, and the residue was redissolved in water/EtOAc. The organic
653 layer was separated, washed with saturated aqueous NaCl, dried over
654 MgSO₄, and filtered. After concentration *in vacuo*, the crude product
655 was purified by flash column chromatography (1:1 EtOAc/hexanes)
656 to yield **5** (35 mg, 35%). *R_f* = 0.2 (1:2 EtOAc/hexanes). ¹H NMR
657 (CDCl₃, 400 MHz): δ_H = 8.37 (s, 1H), 8.21 (d, 1H, *J* = 7.8 Hz), 8.15
658 (br s, 1H), 8.07 (d, 1H, *J* = 7.8 Hz), 7.70–7.63 (m, 3H), 7.37 (t, 2H,
659 *J* = 7.8 Hz), 7.17 (t, 1H, *J* = 7.4 Hz), 4.25 (t, 2H, *J* = 4.5 Hz), 3.71 (t,
660 2H, *J* = 4.5 Hz), 3.59–3.56 (m, 6H), 4.31 (t, 2H, *J* = 4.5 Hz). ¹³C
661 NMR (CDCl₃, 100 MHz): δ_C = 164.07, 137.77, 136.74, 136.55,
662 133.37, 130.89, 130.05, 129.30 (3), 126.28, 125.23, 120.80, 70.85,
663 70.70, 70.16, 70.07, 68.87, 50.81. HRMS (ESI) *m/z* calcd for
664 C₁₉H₂₃N₄O₆ [M + H]⁺ 435.1340, found 435.1344.

665 **Alkynyl Triethoxysilane 7.** Propargylamine (617 mg, 12.12
666 mmol, 3.0 equiv) in toluene (10 mL) was added dropwise to a stirred
667 solution of 3-(triethoxysilyl)propyl isocyanate (1 g, 4.04 mmol, 1.0
668 equiv) in toluene (10 mL) at 0 °C. The reaction mixture was brought
669 to ambient temperature slowly for 2 h and then concentrated to
670 dryness *in vacuo*. The residue was purified by column chromatography
671 (5% MeOH in CH₂Cl₂) to yield **7** (700 mg, 57%). *R_f* = 0.45 (10%
672 MeOH in CH₂Cl₂). ¹H NMR (CDCl₃, 400 MHz): δ_H = 4.66 (br s,
673 1H), 4.58 (br s, 1H), 3.97 (dd, 2H, *J* = 5.5, 2.6 Hz), 3.80 (q, 6H, *J* =
674 13.0, 7.0 Hz), 3.16 (q, 2H, *J* = 13.0, 6.8 Hz), 2.19 (t, 1H, *J* = 2.3 Hz),
675 1.58 (dd, 2H, *J* = 8.2, 6.8 Hz), 1.20 (t, 9H, *J* = 7.0 Hz), 0.62 (t, 2H,
676 *J* = 8.2 Hz). ¹³C NMR (CDCl₃, 100 MHz): δ_C = 158.42, 81.22, 70.93,
677 58.56 (3), 43.01, 30.05, 23.76, 18.41 (3), 7.70. HRMS (APCI) *m/z*
678 calcd for C₁₃H₂₇N₂O₄Si [M + H]⁺ 303.1740, found 303.1738.

679 **Compound 8.** To a solution of **6** (600 mg, 1.67 mmol, 1.0 equiv)
680 in CH₂Cl₂ (10 mL) was added *N*-Boc-1,6-hexanediamine (361 mg,
681 1.67 mmol, 1.0 equiv), EDC·HCl (320 mg, 1.67 mmol, 1.0 equiv),
682 HOBt (225 mg, 1.67 mmol, 1 equiv), and DIPEA (0.58 mL, 3.34
683 mmol, 2.0 equiv). The reaction mixture was stirred at 25 °C for
684 overnight. Water (20 mL) was added to the reaction solution, and
685 then the aqueous phase was extracted with EtOAc (3x30 mL). The
686 organic phase was washed with saturated aqueous NaCl, dried over
687 MgSO₄, filtered, and then concentrated. The crude was purified by
688 flash silica gel column chromatography (3% MeOH in EtOAc/
689 hexanes = 1/1) to give **8** (420 mg, 45%). *R_f* = 0.14 (EtOAc/hexanes =
690 1:1). ¹H NMR (CDCl₃, 400 MHz): δ 8.27 (s, 1H), 8.13 (d, 1H, *J* = 690

691 7.8 Hz), 8.01 (d, 1H, $J = 7.8$ Hz), 7.62 (t, 1H, $J = 7.8$ Hz), 6.66 (br s, 692 1H), 4.54 (br s, 1H), 4.21 (t, 2H, $J = 4.6$ Hz), 3.70 (t, 2H, $J = 4.6$ 693 Hz), 3.61 (t, 2H, $J = 4.8$ Hz), 3.58–3.54 (m, 4H), 3.44 (dd, 2H, $J =$ 694 12.0, 6.0 Hz), 3.34 (t, 2H, $J = 4.8$ Hz), 3.12 (dd, 2H, $J = 12.0, 6.0$ 695 Hz), 1.66–1.60 (m, 2H), 1.51–1.47 (m, 2H), 1.46 (s, 9H), 1.44– 696 1.35 (m, 4H). ^{13}C NMR (CDCl_3 , 100 MHz): δ 165.56, 156.40, 697 136.68, 136.32, 132.87, 130.48, 129.81, 126.36, 70.89, 70.74, 70.22, 698 70.00, 68.87, 50.83, 40.13, 39.97, 30.23 (x2), 29.44, 28.60 (x3), 26.17, 699 25.92. HRMS (ESI) m/z calcd for $\text{C}_{24}\text{H}_{39}\text{N}_3\text{O}_8\text{SNa}$ [$M + \text{H}$] $^+$ 700 580.2417, found 580.2419.

701 **Compound 11.** To a stirred solution of **6** (1.2 g, 3.34 mmol, 1 702 equiv), *N*-hydroxysuccinimide (422 mg, 3.67 mmol, 1.1 equiv), and 703 EDC·HCl (704 mg, 3.67 mmol, 1.1 equiv) in CH_2Cl_2 (15 mL) was 704 added Et_3N (1.02 mL, 7.34 mmol, 2.2 equiv). The reaction mixture 705 was allowed to stir at ambient temperature for 4 h, and then 706 concentrated to dryness *in vacuo*. The residue was dissolved into 707 water (20 mL), and the resulting aqueous layer was extracted with 708 EtOAc (2x30 mL). The combined organic phases were washed with 709 saturated aqueous NaCl, dried over MgSO_4 , filtered, and then 710 concentrated. The residue was purified by flash column chromatog- 711 raphy (1:1 EtOAc /hexanes) to give desired activated ester **11** (310 712 mg, 33%). $R_f = 0.2$ (1:1 EtOAc /hexanes). ^1H NMR (CDCl_3 , 400 713 MHz): $\delta_{\text{H}} = 8.65$ (s, 1H), 8.38 (d, 1H, $J = 7.8$ Hz), 8.21 (d, 1H, $J =$ 714 7.8 Hz), 7.72 (t, 1H, $J = 7.8$ Hz), 4.25 (t, 2H, $J = 4.4$ Hz), 3.70 (t, 2H, 715 $J = 4.4$ Hz), 3.61 (t, 2H, $J = 4.4$ Hz), 3.56–3.54 (m, 4H), 3.33 (t, 2H, 716 $J = 4.4$ Hz), 2.91 (s, 4H). ^{13}C NMR (CDCl_3 , 100 MHz): $\delta_{\text{C}} = 169.00$ 717 (2), 160.52, 137.75, 135.40, 133.89, 130.28, 130.02, 126.77, 70.90, 718 70.74, 70.42, 70.20, 68.78, 50.79, 25.82 (2). HRMS (ESI) m/z calcd 719 for $\text{C}_{17}\text{H}_{20}\text{N}_4\text{O}_9\text{SNa}$ [$M + \text{Na}$] $^+$ 479.0849, found 479.0841.

720 **Compound 12.** DIPEA (0.292 mL, 1.68 mmol, 2.0 equiv) was 721 added to a solution of 6-[(6-[[*tert*-butoxycarbonyl]amino]hexanoyl)- 722 amine]hexanoic acid (289 mg, 0.84 mmol, 1.0 equiv), amine **9** (480 723 mg, 0.84 mmol, 1.0 equiv), EDC·HCl (161 mg, 0.84 mmol, 1.0 724 equiv), and HOBt (113 mg, 0.84 mmol, 1.0 equiv) in CH_2Cl_2 (20 725 mL). The reaction mixture was allowed to stir at ambient temperature 726 for 12 h. The reaction mixture was then concentrated *in vacuo*, and 727 the resulting residue was redissolved in water/ EtOAc . The organic 728 layer was separated, washed with saturated aqueous NaCl, dried over 729 MgSO_4 , and filtered. After concentration *in vacuo*, the crude product 730 was purified by flash column chromatography (2–5% MeOH in 731 CH_2Cl_2) to yield **12** (310 mg, 65%). $R_f = 0.35$ (10% MeOH in 732 CH_2Cl_2). ^1H NMR (CDCl_3 , 400 MHz): $\delta_{\text{H}} = 8.33$ (s, 1H), 8.17 (d, 733 1H, $J = 7.8$ Hz), 8.01 (d, 1H, $J = 7.8$ Hz), 7.61 (t, 1H, $J = 7.8$ Hz), 734 7.14 (br s, 1H), 5.81 (br s, 1H), 5.71 (br s, 1H), 4.62 (br s, 1H), 4.19 735 (t, 2H, $J = 4.6$ Hz), 3.68 (t, 2H, $J = 4.6$ Hz), 3.61 (t, 2H, $J = 4.6$ Hz), 736 3.58–3.54 (m, 4H), 3.43 (dd, 2H, $J = 12.0, 6.0$ Hz), 3.34 (t, 2H, $J =$ 737 4.6 Hz), 3.26–3.18 (m, 4H), 3.06 (dd, 2H, $J = 12.0, 6.0$ Hz), 2.17– 738 2.10 (m, 4H), 1.59–1.55 (m, 4H), 1.51–1.42 (m, 10H), 1.40 (s, 9H), 739 1.37–1.26 (m, 6H). ^{13}C NMR (CDCl_3 , 100 MHz): $\delta_{\text{C}} = 173.42$, 740 173.29, 165.68, 156.29, 136.53, 136.39, 132.99, 130.35, 129.70, 741 126.64, 70.85, 70.70, 70.18, 70.00 68.83, 50.80, 39.91, 39.26, 38.94, 742 36.67 (2), 36.54, 29.91, 29.82, 29.63, 29.37, 29.34, 28.57 (3), 26.46, 743 26.11, 26.00, 25.52, 25.35 (2). HRMS (ESI) m/z calcd for 744 $\text{C}_{36}\text{H}_{61}\text{N}_7\text{O}_{10}\text{SNa}$ [$M + \text{Na}$] $^+$ 806.4098, found 806.4088.

745 **Materials Characterization.** X-ray photoelectron spectroscopy 746 measurements were performed using a PHI Quantera SXM (ULVAC- 747 PHI, Japan) high-resolution spectrometer. A monochromatized Al 748 anode was used as the excitation source. The C 1s (C–C) peak at 749 283.5 eV was chosen as the reference line. Surface morphologies of 750 the BA–phenylsulfonate ester (**2**)-coated glass slides before and after 751 IgG microarray fabrication were characterized using an atomic force 752 microscope (Bruker Multimode 8). The ToF-SIMS data were 753 acquired on a TOF-SIMS 5 instrument (ION-TOF GmbH, Münster, 754 Germany) using a Bi^{3+} primary ion source.

755 **Preparation of Mixed Monolayer-Protected Alkynylated** 756 **Glass Slides.** FEA microscope plain slides with ground edges (1.2 757 mm, 1" × 3") were thoroughly cleaned using a freshly prepared 758 piranha solution (three parts 18 M H_2SO_4 and one part 30% H_2O_2) 759 for 1 h and then successively rinsed with deionized water and ethanol 760 prior to use (Caution! Wear suitable protective apparel when handling

highly corrosive acids). A pre-mixed solution of alkynyl siloxane **7** (10 761 mM, DMSO) and freshly prepared aqueous solution of SBS at 10:1 762 molar ratio was applied to the glass slide and allowed to form a mixed 763 monolayer for 6 h at room temperature (rt). A 16-well incubation 764 chamber (Sigma-Aldrich) was applied to prevent cross-contamination 765 between two different wells. The alkynylated slides were washed with 766 DMSO and deionized water for 10 min each followed by drying under 767 centrifugation. The dried slides could be stored until use. 768

769 **Preparation of BA–Phenylsulfonate Ester-Coated Glass** 770 **Slides through CuAAC Reaction.** A 100 μL solution of BA– 771 phenylsulfonate ester probes (10 mM, 3:1 DMSO/ H_2O ratio) was 772 applied to the alkynylated glass slides with the help of a 16-well 773 incubation chamber followed by addition of a pre-mixed aqueous 774 solution of catalyst (final concentration of $\text{CuSO}_4 \cdot 5\text{H}_2\text{O}$ at 100 μM , 775 THPTA at 200 μM , and sodium ascorbate at 100 μM). The solution 776 was mixed properly with a pipette and allowed to react for 12 h at 777 room temperature. The slides were rinsed with DMSO, washed with 778 phosphate-buffered saline (PBS, pH 7.4), and finally dried by 779 centrifugation. The BA–phenylsulfonate ester-coated slides could be 780 stored in a desiccator until further use.

781 **Microarray Fabrication and Preparation.** The Ab microarrays 782 were prepared by modification of previously described procedures.³² 783 Approximately 0.6 nL of monoclonal capture Abs (1.6 μM) in 20 mM 784 HEPES buffer (containing 150 mM NaCl and 0.005% Tween20, pH 785 8.5) was respectively dispensed using a robotic contact arrayer 786 (AD1500 Arrayer, BioDot) fitted with Stealth Pins SMP3 (ArrayIt 787 Corporation) onto BA–phenylsulfonate ester functionalized glass 788 slides. The printing process was performed at a relative humidity of 789 84%, and the temperature was maintained below 26 °C. The slides 790 were then incubated in a microarray hybridization chamber (CamLab, 791 UK) at ambient temperature for 12 h followed by sequential washing 792 with phosphate-buffered saline (PBS), PBS with 0.005% Tween20 793 (PBST), and deionized H_2O for 5 min each under gentle shaking to 794 remove any unbound Abs. The remaining BAs on the surface were 795 then blocked with a 100 μM solution of dextran containing 1% BSA in 796 water at room temperature for 2 h to prevent nonspecific adhesion/ 797 interactions. After washing, the oriented Ab immobilized microarray 798 slides could be probed with an anti-h IgG Fc-specific Cy3-labeled Ab 799 for direct interrogation of h-IgG or in a layer-by-layer format for 800 cognate analyte-binding studies. The printed slides could be stored at 801 4 °C until use.

802 **Antibody-Microarray Assays and Data Analysis.** A 100 μL 803 portion of each sample solution in assay buffer (PBS buffer containing 804 0.005% Tween20 and 0.1% BSA, pH 7.4) was incubated on each array 805 for 1 h at room temperature. Captured antigens were detected with 806 biotinylated Abs at a concentration of 1 $\mu\text{g}/\text{mL}$ in assay buffer 807 followed by incubation with streptavidin-Cy3 (10 $\mu\text{g}/\text{mL}$) using 808 incubation and wash conditions as mentioned above. The slides were 809 scanned for fluorescence image acquisition using a Revolution 4550 810 scanner (Vidar Corp., USA) or SpinScan Microarray Scanner HC- 811 BS01 (Caduceus Biotechnology Inc.) with a Cy3 filter. The 812 fluorescence intensity of the spots was quantified using the 813 ArrayVision software package (version 8.0) with correction for local 814 background. All proteins were analyzed in triplicate; the data 815 represented an average of 18–20 spots for a given antigen 816 concentration. The mean intensity of each spot was taken as a single 817 data point for analysis.

■ ASSOCIATED CONTENT

Supporting Information

The Supporting Information is available free of charge at 820 <https://pubs.acs.org/doi/10.1021/acsabm.0c00700>. 821

General procedure, synthesis of **6** and **10**, additional 822 details corresponding to Figures S1–S13, and NMR 823 spectra of all new compounds (PDF) 824

825 ■ AUTHOR INFORMATION

826 Corresponding Authors

827 Avijit K. Adak – Department of Chemistry, National Tsing Hua
828 University, Hsinchu 300, Taiwan; Email: akadak@
829 mx.nthu.edu.tw

830 Chun-Cheng Lin – Department of Chemistry, National Tsing
831 Hua University, Hsinchu 300, Taiwan; Department of
832 Medicinal and Applied Chemistry, Kaohsiung Medical
833 University, Kaohsiung 80708, Taiwan;  [orcid.org/0000-
834 0002-2323-0920](https://orcid.org/0000-0002-2323-0920); Email: cclin66@mx.nthu.edu.tw

835 Authors

836 Kuan-Ting Huang – Department of Chemistry, National Tsing
837 Hua University, Hsinchu 300, Taiwan

838 Pei-Jhen Li – Department of Chemistry, National Tsing Hua
839 University, Hsinchu 300, Taiwan

840 Chen-Yo Fan – Department of Chemistry, National Tsing Hua
841 University, Hsinchu 300, Taiwan

842 Po-Chiao Lin – Department of Chemistry, National Sun Yat-sen
843 University, Kaohsiung 804, Taiwan

844 Kuo-Chu Hwang – Department of Chemistry, National Tsing
845 Hua University, Hsinchu 300, Taiwan;  [orcid.org/0000-
846 0003-1814-9869](https://orcid.org/0000-0003-1814-9869)

847 Complete contact information is available at:

848 <https://pubs.acs.org/10.1021/acsabm.0c00700>

849 Author Contributions

850 The manuscript was written through contributions of all
851 authors. All authors have given approval to the final version of
852 the manuscript.

853 Notes

854 The authors declare no competing financial interest.

855 ■ ACKNOWLEDGMENTS

856 This work was financially supported by the National Tsing
857 Hua University, Academia Sinica (AS-TP-108-M06), the
858 Ministry of Science and Technology (107-2113-M-007-024-
859 MY3), the Ministry of Education of Taiwan, MOST
860 Instrument Center at NTHU, and Frontier Research Center
861 on Fundamental and Applied Sciences of Matters.

862 ■ REFERENCES

863 (1) Sliwkowski, M. X.; Mellman, I. Antibody Therapeutics in
864 Cancer. *Science* **2013**, *341*, 1192–1198.
865 (2) Haab, B. B. Applications of Antibody Array Platforms. *Curr.*
866 *Opin. Biotechnol.* **2006**, *17*, 415–421.
867 (3) Vashist, S. K.; Lam, E.; Hrapovic, S.; Male, K. B.; Luong, J. H. T.
868 Immobilization of Antibodies and Enzymes on 3-Aminopropyltri-
869 thoxysilane-Functionalized Bioanalytical Platforms for Biosensors and
870 Diagnostics. *Chem. Rev.* **2014**, *114*, 11083–11130.
871 (4) Shen, M.; Rusling, J. F.; Dixit, C. K. Site-selective Orientated
872 Immobilization of Antibodies and Conjugates for Immunodiagnos-
873 tics Development. *Methods* **2017**, *116*, 95–111.
874 (5) Hermanson, G. T. *Bioconjugate techniques* (3rd Ed.); Elsevier Inc.,
875 2013.
876 (6) Kausaite-Minkstimiene, A.; Ramanaviciene, A.; Kirlyte, J.;
877 Ramanavicius, A. Comparative Study of Random and Oriented
878 Antibody Immobilization Techniques on the Binding Capacity of
879 Immunosensor. *Anal. Chem.* **2010**, *82*, 6401–6408.
880 (7) Trilling, A. K.; Beekwilder, J.; Zuilhof, H. Antibody Orientation
881 on Biosensor Surfaces: a Minireview. *Analyst* **2013**, *138*, 1619–1627.
882 (8) Karyakin, A. A.; Presnova, G. V.; Rubtsova, M. Y.; Egorov, A. M.
883 Oriented Immobilization of Antibodies onto the Gold Surfaces via
884 Their Native Thiol Groups. *Anal. Chem.* **2000**, *72*, 3805–3811.

(9) van Buren, N.; Rehder, D.; Gadgil, H.; Matsumura, M.; Jacob, J. 885
Elucidation of Two Major Aggregation Pathways in an IgG2 886
Antibody. *J. Pharm. Sci.* **2009**, *98*, 3013–3030. 887

(10) Seo, J. S.; Lee, S.; Poulter, C. D. Regioselective Covalent 888
Immobilization of Recombinant Antibody-Binding Proteins A, G, and 889
L for Construction of Antibody Arrays. *J. Am. Chem. Soc.* **2013**, *135*, 890
8973–8980. 891

(11) Jung, Y.; Lee, J. M.; Kim, J. W.; Yoon, J.; Cho, H.; Chung, B. H. 892
Photoactivable Antibody Binding Protein: Site-Selective and Covalent 893
Coupling of Antibody. *Anal. Chem.* **2009**, *81*, 936–942. 894

(12) Konrad, A.; Karlström, A. E.; Hober, S. Covalent 895
Immunoglobulin Labeling through a Photoactivable Synthetic Z 896
Domain. *Bioconjugate Chem.* **2011**, *22*, 2395–2403. 897

(13) Lee, Y.; Jeong, J.; Lee, G.; Moon, J. H.; Lee, M. K. Covalent 898
and Oriented Surface Immobilization of Antibody Using Photo- 899
activatable Antibody Fc-Binding Protein Expressed in *Escherichia coli*. 900
Anal. Chem. **2016**, *88*, 9503–9509. 901

(14) Kumar, S.; Aaron, J.; Sokolov, K. Directional Conjugation of 902
Antibodies to Nanoparticles for Synthesis of Multiplexed Optical 903
Contrast Agents With Both Delivery and Targeting Moieties. *Nat.* 904
Protoc. **2008**, *3*, 314–320. 905

(15) Duval, F.; van Beek, T. A.; Zuilhof, H. Key Steps Towards the 906
Oriented Immobilization of Antibodies Using Boronic Acids. *Analyst* 907
2015, *140*, 6467–6472. 908

(16) Jefferis, R. Glycosylation as a Strategy to Improve Antibody- 909
Based Therapeutics. *Nat. Rev. Drug Discovery* **2009**, *8*, 226–234. 910

(17) Sun, X.; Zhai, W.; Fossey, J. S.; James, T. D. Boronic Acids for 911
Fluorescence Imaging of Carbohydrates. *Chem. Commun.* **2016**, *52*, 912
3456–3469. 913

(18) Matsumoto, A.; Cabral, H.; Sato, N.; Kataoka, K.; Miyahara, Y. 914
Assessment of Tumor Metastasis by the Direct Determination of Cell- 915
Membrane Sialic Acid Expression. *Angew. Chem., Int. Ed.* **2010**, *49*, 916
5494–5497. 917

(19) Ellis, G. A.; Palte, M. J.; Raines, R. T. Boronate-Mediated 918
Biologic Delivery. *J. Am. Chem. Soc.* **2012**, *134*, 3631–3634. 919

(20) Liu, H.; Li, Y.; Sun, K.; Fan, J.; Zhang, P.; Meng, J.; Wang, S.; 920
Jiang, L. Dual-Responsive Surfaces Modified with Phenylboronic 921
Acid-Containing Polymer Brush To Reversibly Capture and Release 922
Cancer Cells. *J. Am. Chem. Soc.* **2013**, *135*, 7603–7609. 923

(21) Akgun, B.; Hall, D. G. Fast and Tight Boronate Formation for 924
Click Bioorthogonal Conjugation. *Angew. Chem., Int. Ed.* **2016**, *55*, 925
3909–3913. 926

(22) Bao, L.; Ding, L.; Yang, M.; Ju, H. Noninvasive imaging of 927
sialyltransferase activity in living cells by chemoselective recognition. 928
Sci. Rep. **2015**, DOI: [10.1038/srep10947](https://doi.org/10.1038/srep10947). 929

(23) Li, L.; Lu, Y.; Bie, Z.; Chen, H. Y.; Liu, Z. Photolithographic 930
Boronate Affinity Molecular Imprinting: a General and Facile 931
Approach for Glycoprotein Imprinting. *Angew. Chem., Int. Ed.* **2013**, 932
52, 7451–7454. 933

(24) Moreno-Guzmán, M.; Ojeda, I.; Villalonga, R.; González- 934
Cortés, A.; Yáñez-Sedeño, P.; Pingarrón, J. M. Ultrasensitive 935
Detection of Adrenocorticotropin Hormone (ACTH) Using Dis- 936
posable Phenylboronic-Modified Electrochemical Immunosensors. 937
Biosens. Bioelectron. **2012**, *35*, 82–86. 938

(25) Song, L.; Zhao, J.; Luan, S.; Ma, J.; Liu, J.; Xu, X.; Yin, J. 939
Fabrication of a Detection Platform with Boronic-Acid-Containing 940
Zwitterionic Polymer Brush. *ACS Appl. Mater. Interfaces* **2013**, *5*, 941
13207–13215. 942

(26) Song, H. Y.; Hogley, J.; Su, X.; Zhou, X. End-on Covalent 943
Antibody Immobilization on Dual Polarization Interferometry Sensor 944
Chip for Enhanced Immuno-sensing. *Plasmonics* **2014**, *9*, 851–858. 945

(27) Abad, J. M.; Vélez, M.; Santamaría, C.; Guisán, J. M.; Matheus, 946
P. R.; Vázquez, L.; Gazaryan, I.; Gorton, L.; Gibson, T.; Fernández, V. 947
M. Immobilization of Peroxidase Glycoprotein on Gold Electrodes 948
Modified with Mixed Epoxy-Boronic Acid Monolayers. *J. Am. Chem.* 949
Soc. **2002**, *124*, 12845–12853. 950

(28) Adak, A. K.; Li, B.-Y.; Huang, L.-D.; Lin, T.-W.; Chang, T.-C.; 951
Huang, K. C.; Lin, C.-C. Fabrication of Antibody Microarrays by 952

- 953 Light-Induced Covalent and Oriented Immobilization. *ACS Appl. Mater. Interfaces* **2014**, *6*, 10452–10460.
- 955 (29) Fan, C.-Y.; Hou, Y.-R.; Adak, A. K.; Waniwan, J. T.; dela Rosa, M. A. C.; Low, P. Y.; Angata, T.; Hwang, K.-C.; Chen, Y.-J.; Lin, C.-C. Boronate Affinity-Based Photoactivatable Magnetic Nanoparticles for the Oriented and Irreversible Conjugation of Fc-Fused Lectins and Antibodies. *Chem. Sci.* **2019**, *10*, 8600–8609.
- 960 (30) Chen, M.-L.; Adak, A. K.; Yeh, N.-C.; Yang, W.-B.; Chuang, Y.-J.; Wong, C.-H.; Hwang, K.-C.; Hwu, J.-R. R.; Hsieh, S.-L.; Lin, C.-C. Fabrication of an Oriented Fc-Fused Lectin Microarray through Boronate Formation. *Angew. Chem., Int. Ed.* **2008**, *47*, 8627–8630.
- 964 (31) Lin, P.-C.; Chen, S.-H.; Wang, K.-Y.; Chen, M.-L.; Adak, A. K.; Hwu, J.-R. R.; Chen, Y.-J.; Lin, C.-C. Fabrication of Oriented Antibody-Conjugated Magnetic Nanoparticles and Their Immunoaffinity Application. *Anal. Chem.* **2009**, *81*, 8774–8782.
- 968 (32) Huang, L.-D.; Adak, A. K.; Yu, C.-C.; Hsiao, W.-C.; Lin, H.-J.; Chen, M.-L.; Lin, C.-C. Fabrication of Highly Stable Glyco-Gold Nanoparticles and Development of a Glyco-Gold Nanoparticle-Based Oriented Immobilized Antibody Microarray for Lectin (GOAL) Assay. *Chem. – Eur. J.* **2015**, *21*, 3956–3967.
- 973 (33) Akgun, B.; Hall, D. G. Boronic Acids as Bioorthogonal Probes for Site-Selective Labeling of Proteins. *Angew. Chem., Int. Ed.* **2018**, *57*, 13028–13044.
- 976 (34) Tsukiji, S.; Miyagawa, M.; Takaoka, Y.; Tamura, T.; Hamachi, I. Ligand-Directed Tosyl Chemistry for Protein Labeling *in vivo*. *Nat. Chem. Biol.* **2009**, *5*, 341–343.
- 979 (35) Yang, Y.-L.; Lee, Y.-P.; Yang, Y.-L.; Lin, P.-C. Traceless Labeling of Glycoproteins and Its Application to the Study of Glycoprotein–Protein Interactions. *ACS Chem. Biol.* **2014**, *9*, 390–397.
- 983 (36) Tu, H.-C.; Lee, Y.-P.; Liu, X.-Y.; Chang, C.-F.; Lin, P.-C. Direct Screening of Glycan Patterns from Human Sera: A Selective Glycoprotein Microarray Strategy. *ACS Appl. Biomater.* **2019**, *2*, 1286–1297.
- 987 (37) Schlenoff, J. B. Zwitterion-Coating Surfaces with Zwitterionic Functionality to Reduce Nonspecific Adsorption. *Langmuir* **2014**, *30*, 9625–9636.
- 990 (38) Khanal, M.; Vausselin, T.; Barras, A.; Bande, O.; Turcheniuk, K.; Benazza, M.; Zaitsev, V.; Teodorescu, C. M.; Boukherroub, R.; Siriwardena, A.; Dubuisson, J.; Szunerits, S. Phenylboronic-Acid-Modified Nanoparticles: Potential Antiviral Therapeutics. *ACS Appl. Mater. Interfaces* **2013**, *5*, 12488–12498.
- 995 (39) Zhang, X.; He, X.; Chen, L.; Zhang, Y. Boronic Acid Modified Magnetic Nanoparticles for Enrichment of Glycoproteins *via* Azide and Alkyne Click Chemistry. *J. Mater. Chem.* **2012**, *22*, 16520–16526.
- 998 (40) Chan, T. R.; Hilgraf, R.; Sharpless, K. B.; Fokin, V. V. Polytriazoles as Copper(I)-Stabilizing Ligands in Catalysis. *Org. Lett.* **2004**, *6*, 2853–2855.
- 1001 (41) Paslaru, E.; Baican, M. C.; Hitruc, E. G.; Nistor, M. T.; Epailard, F. P.; Vasile, C. Immunoglobulin G Immobilization on PVDF Surface. *Colloids Surf., B* **2014**, *115*, 139–149.
- 1004 (42) Foster, R. N.; Harrison, E. T.; Castner, D. G. ToF-SIMS and XPS Characterization of Protein Films Adsorbed onto Bare and Sodium Styrenesulfonate-Grafted Gold Substrates. *Langmuir* **2016**, *32*, 3207–3216.
- 1008 (43) Kim, J.; Cho, J.; Seidler, P. M.; Kurland, N. E.; Yadavalli, V. K. Investigations of Chemical Modification of Amino-Terminated Organic Films on Silicon Substrates and Controlled Protein Immobilization. *Langmuir* **2010**, *26*, 2599–2608.
- 1012 (44) Chen, H.; Huang, J.; Lee, J.; Hwang, S.; Koth, K. Surface Plasmon Resonance Spectroscopic Characterization of Antibody Orientation and Activity on the Calixarene Monolayer. *Sens. Actuators B* **2010**, *147*, 548–553.
- 1016 (45) Wang, H.; Castner, D. G.; Ratner, B. D.; Jiang, S. Probing the Orientation of Surface-Immobilized Immunoglobulin G by Time-of-Flight Secondary Ion Mass Spectroscopy. *Langmuir* **2004**, *20*, 1877–1887.
- 1020 (46) Liu, F.; Dubey, M.; Takahashi, H.; Castner, D. G.; Grainger, D. W. Immobilized Antibody Orientation Analysis Using Secondary Ion Mass Spectroscopy and Fluorescence Imaging of Affinity-Generated Patterns. *Anal. Chem.* **2010**, *82*, 2947–2958.
- 1023 (47) Welch, N. G.; Scoble, J. A.; Muir, B. W.; Pigram, P. J. Orientation and Characterization of Immobilized Antibodies for Improved Immunoassays. *Biointerphases* **2017**, *12*, No. 02D301.
- 1026 (48) Ludwig, J. A.; Weinstein, J. N. Biomarkers in Cancer Staging, Prognosis and Treatment Selection. *Nat Rev Cancer* **2005**, *5*, 845–856.
- 1029 (49) Du Clos, T. W. Pentraxins: Structure, Function, and Role in Inflammation. *ISRN Inflammation* **2013**, *2013*, 379040.
- 1031 (50) Pepys, M. B.; Dash, A. C.; Markham, R. E.; Thomas, H. C.; Williams, B. D.; Petrie, A. Comparative Clinical Study of Protein SAP (amyloid P component) and C-reactive Protein in Serum. *Clin. Exp. Immunol.* **1978**, *32*, 119–124.
- 1035 (51) Clyne, B.; Olshaker, J. S. The C-reactive Protein. *J. Emerg. Med.* **1999**, *17*, 1019–1025.
- 1037 (52) Ridker, P. M.; Rifai, N.; Rose, L.; Buring, J. E.; Cook, N. R. Comparison of C-reactive Protein and Low-Density Lipoprotein Cholesterol Levels in the Prediction of First Cardiovascular Events. *N. Engl. J. Med.* **2002**, *347*, 1557–1565.
- 1041 (53) Laurent, P.; Marchand, B.; Bienvenu, J.; Marichy, J. Rapid Enzyme Immunoassay for Quantification of C-reactive Protein (CRP). *Clin. Biochem.* **1985**, *18*, 272–275.
- 1044 (54) Kingsmore, S. F. Multiplexed Protein Measurement: Technologies and Applications of Protein and Antibody Arrays. *Nat Rev Drug Discov.* **2006**, *5*, 310–321.
- 1047 (55) Juncker, D.; Bergeron, S.; Laforte, V.; Li, H. Cross-reactivity in Antibody Microarrays and Multiplexed Sandwich Assays: Shedding Light on the Dark Side of Multiplexing. *Curr. Opin. Chem. Biol.* **2014**, *18*, 29–37.
- 1051